

# Macroscopic Photocontrol of Ion-Transporting Pathways of a Nanostructured Imidazolium-Based Photoresponsive Liquid Crystal

Bartolome Soberats,<sup>†,‡</sup> Emi Uchida,<sup>†,‡</sup> Masafumi Yoshio,<sup>†</sup> Junko Kagimoto,<sup>§</sup> Hiroyuki Ohno,<sup>§</sup> and Takashi Kato<sup>\*,†</sup>

<sup>†</sup>Department of Chemistry and Biotechnology, School of Engineering, The University of Tokyo, Hongo, Bunkyo-ku, Tokyo 113-8656, Japan

<sup>§</sup>Department of Biotechnology, Tokyo University of Agriculture and Technology, Nakacho, Koganei, Tokyo 184-8588, Japan

**S** Supporting Information

**ABSTRACT:** The photocontrol of the macroscopic alignment of nanostructured 2D ion-transporting pathways is described. The uniplanar homogeneous alignment of the thermotropic smectic (Sm) liquid-crystalline (LC) phase has been successfully achieved via photoinduced reorientation of the azobenzene groups of the imidazolium-based LC material. The ionic layers of the Sm LC phase are macroscopically oriented perpendicular to the surface of the glass substrate. The oriented films show anisotropic ion conduction in the Sm phase. This is the first example of the macroscopic photoalignment of ion-conductive LC arrays. Reversible switching of homeotropic and homogeneous alignments has also been achieved for the LC material. These materials and the alignment methodology may be useful in the development of ion-based circuits and memory devices.

Self-assembled ionic soft materials have attracted a great deal of attention due to their ability to form nanostructured and well-defined ion channels.<sup>1,2</sup> The use of ionic liquid crystals<sup>1</sup> has been found to be a versatile approach for the development of ion transporting materials forming 1D,<sup>3</sup> 2D,<sup>4</sup> and 3D<sup>5</sup> ionic pathways. Among these materials, columnar and smectic (Sm) assemblies are of interest for ion transportation in a specific desired direction.<sup>3,4,6</sup> Anisotropic ion conductors may be applicable to the development of ionic devices such as batteries and ion transistors. However, the orientation of liquid-crystalline (LC) domains to the specific direction is still challenging. To date, the macroscopic alignment of ion-based thermotropic liquid crystals has been achieved in columnar hexagonal and Sm LC phases by the application of shear force,<sup>3,4</sup> electric field,<sup>7</sup> rubbing treatment,<sup>8</sup> and surface modification.<sup>3b</sup> These methods require the physical contact with the samples or the use of specific substrates which are not always compatible for their use in practical applications.<sup>9</sup>

Therefore, the development of more useful methodologies for the alignment of ion-transporting pathways is particularly attractive for the preparation of efficient LC devices. Our approach here is to develop stimuli responsive ion-conductive LC materials.<sup>10</sup> Herein we report on the photoinduced orientation of 2D ion-transporting nanopathways (Figure 1). Homogeneously aligned LC thin films of photoresponsive compound **1** (Figure 1a) have been successfully obtained via

the axis selective *cis-to-trans* photoisomerization of azobenzene (Azo) groups by using linearly polarized (LP) visible light irradiation (Figure 1b). This change in pathway alignment between parallel (homeotropic) and perpendicular (homogeneous) to the substrate is reversible. Ion-conductive measurements confirmed the anisotropic nature of the ion transport in the photoaligned arrays.

We have designed and prepared imidazolium-based wedge-shaped LC molecule **1** bearing three Azo groups (Figure 1a). We expected that the photoinduced reorientation of the Azo moieties (Figure 1b) in **1** led to the orientation of ion-transporting pathways, which significantly simplifies the alignment process. Compound **1** was expected to show an Sm phase.<sup>11</sup> We aimed to achieve the macroscopic photoalignment of the 2D ionic pathways perpendicular to the surface of the substrate. This photocontrol is of interest for their efficient application as electrolytes in sandwiched devices.<sup>9</sup> The alignment of bulk materials driven by the photoinduced orientation of Azo groups was reported.<sup>12</sup> This approach was shown to be useful in the orientation of ionic LC arrays.<sup>2f,13</sup> However, to our knowledge no photoalignment was reported for LC ion-transporting materials.

Compound **1** was isolated as a yellow-orange solid, which exhibited thermotropic LC phases upon heating. The LC behavior of **1** was examined by polarizing optical microscopy (POM), differential scanning calorimetry, and powder X-ray diffraction (XRD) measurements. Imidazolium salt **1** exhibited an enantiotropic smectic A (SmA) phase from 95 to 140 °C and a nematic (N) phase from 140 until 149 °C in a heating process (Figure 1 and Supporting Information). Compound **1** spontaneously aligned homeotropically on glass and quartz substrates after cooling from isotropic to LC and solid states (Figure 1b top). The XRD pattern of compound **1** at 120 °C showed two intense peaks at 21.4 and 14.2 Å, which were assigned to the (002) and (003) diffraction peaks of an SmA phase (Supporting Information). On the other hand, the XRD pattern at 145 °C only showed a diffused halo peak. This phase was identified as an N phase according to the POM observation (Supporting Information). Normally, ionic liquid crystals exhibit nanosegregated LC phases such as Sm and columnar phases due their block structures consisting of ionic and

Received: April 26, 2014

Published: June 24, 2014

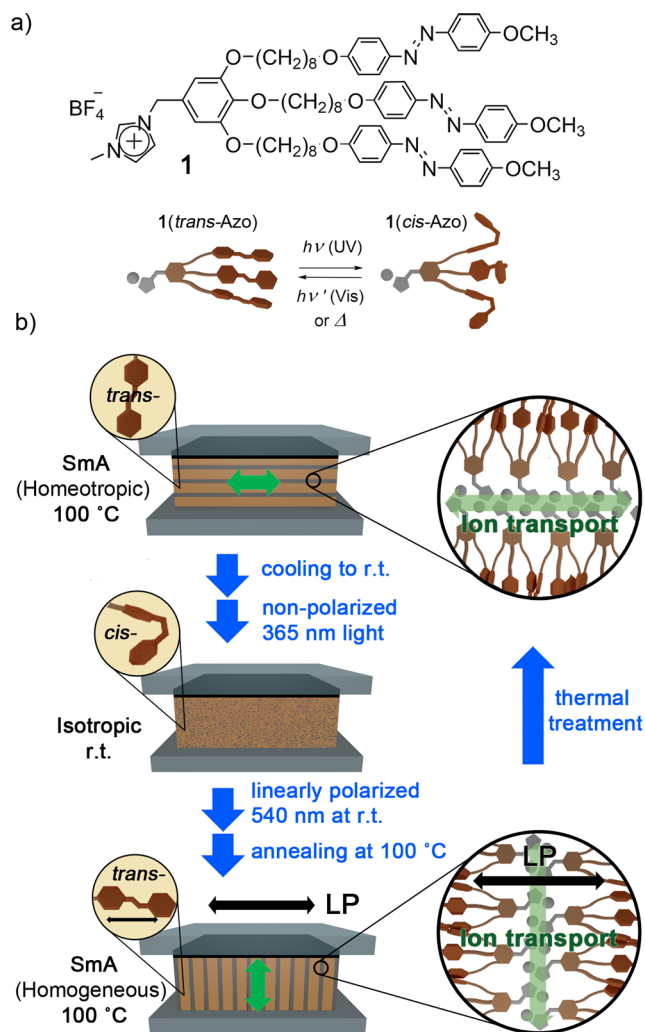


**Figure 1.** (a) Molecular structure of compound **1**. Schematic representation of the Azobenzene (Azo) *trans-cis* isomerization in **1** (bottom). (b) Schematic representation of the photoinduced reorientation of liquid-crystalline thin films of **1**. Insets show the molecular assembly. Direction of ion transporting 2D channels marked in green arrows. Direction of the linearly polarized (LP) light marked as black arrows. SmA: smectic A; N: nematic; Iso: isotropic.

nonionic moieties.<sup>1</sup> For compound **1**, the N phase is formed because of the lower weight fraction of ionic parts. In this case, the nonionic flexible folk-like mesogenic part dominates the liquid crystalline behavior in this higher temperature range, which results in the formation of the N phase (Supporting Information).

The photoorientation method by the axis selective *cis-to-trans* photoisomerization of Azo is especially effective to align polymeric LC materials,<sup>14</sup> and it consists of exposing a *cis*-Azo-based photostationary state to LP visible light (Supporting Information).<sup>14</sup> This method was successfully applied for the selective homogeneous alignment of ionic thin films of **1** (Figure 1b and Supporting Information).<sup>14,15</sup> The exposure of the homeotropically aligned thin film of **1** (Figure 1b top) to 360 nm UV light induced the *trans-to-cis* isomerization of Azo groups, which led to a viscous isotropic phase (Figure 1b middle). The further exposure of the film to LP 540 nm visible light induced the *cis-to-trans* photoisomerization where the Azo molecules were oriented parallel to the linear polarizer. After the subsequent thermal annealing of the film at 100 °C in the

SmA phase, these processes resulted in the homogeneous alignment of the lamellar structure of LC **1** with the ionic layers perpendicular to the LP light (Figure 1b, bottom). Remarkably, this process was reversible. After heating to the isotropic state followed by the slow cooling to the SmA phase, **1** recovered the initial homeotropic organization (Figure 1b and Supporting Information).

The alignment of the thin film of **1** after the Azo photoreorientation process<sup>15</sup> was examined by polarized UV-vis absorption spectroscopy, and the results are shown in Figure 2a. An intense absorption band of the *trans*-Azo is observed at

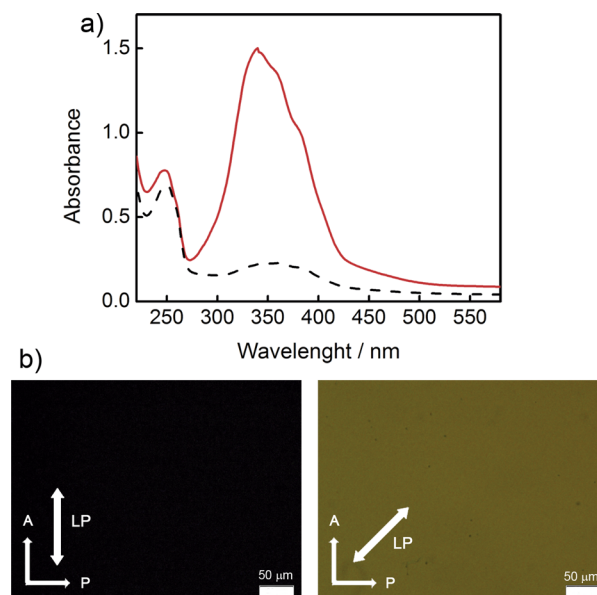


**Figure 2.** (a) Polarized UV-vis absorption spectra of photoaligned thin film of **1**, parallel (red) and perpendicular (black dashed) to the direction of the LP light previously applied for the alignment. (b) Polarizing optical microscopic images of photoaligned film of **1** at 100 °C in the SmA phase. The direction of the linearly polarized (LP) light irradiated in the alignment of the film is (left) parallel to the direction of the microscope analyzer (A) and (right) after rotation by 45° with respect to the analyzer (A). Directions of the analyzer (A), polarizer (P), and the polarized light (LP) used for the photoalignment are indicated with white arrows.

340 nm when the polarizer is parallel to the direction of the LP light applied on the film. However, this band drastically decreases after rotation of the polarizer by 90°. These results suggest that the *trans*-Azo groups are aligned parallel to the direction of the applied LP light (Figure 1b bottom). The POM observation of the irradiated thin films (Figure 2b) has confirmed that the reorientation of Azo groups successfully results in the uniplanar alignment of the LC domains (Figure 1b bottom). The POM images of the aligned thin film of **1** in the SmA phase show no birefringence when the polarizer or analyzer is parallel to the direction of the applied LP (Figure 2b, left). However, after rotation of the sample holder by 45° the image becomes homogeneously colored, indicating the macroscopic homogeneous alignment of the SmA phase (Figure 2b, right). Thus, the UV-vis absorption spectroscopy measurements and the POM images (Figure 2) together have confirmed the macroscopic orientation of the lamellar structures of **1** where the Azo groups are aligned parallel to the LP light irradiation and the ionic layers lies perpendicular to

the surface of the substrate and to the applied LP light (Figure 1b, bottom).

Thin films of **1** were prepared and photoaligned on glass cells with comb-shaped gold electrodes, and their ionic conductivities were measured (Supporting Information).<sup>15,16</sup> Figure 3a

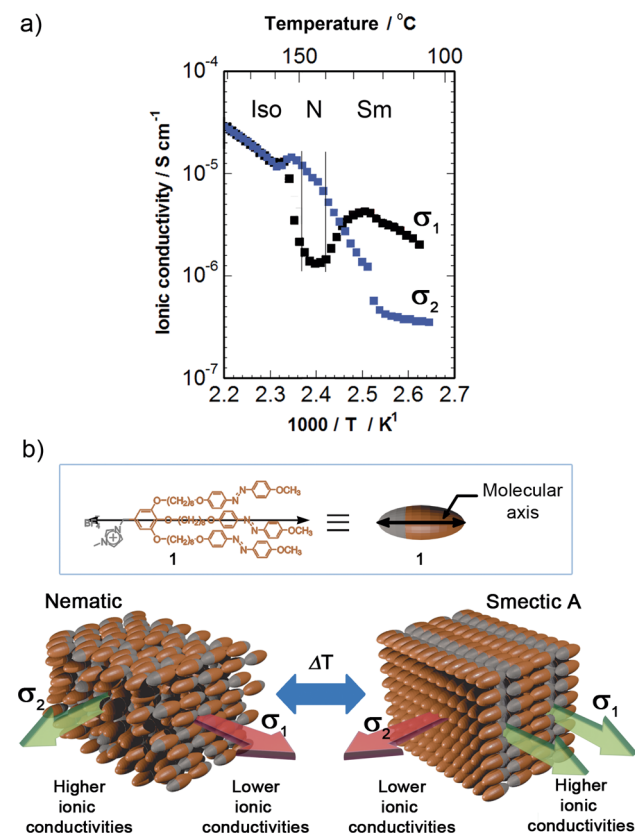


**Figure 3.** (a) Ionic conductivities of aligned samples of **1** as a function of the temperature in the perpendicular ( $\sigma_1$ ) (black) and the parallel ( $\sigma_2$ ) (blue) directions of the molecular axis. (b) Schematic illustration of the homogeneous alignments of **1** in the N (left) and SmA (right) phases. The direction of ion transport is represented with green (higher conductivities) and red (lower conductivities) arrows. Interdigitation between molecules is omitted for clarity.

shows the ionic conductivities ( $\sigma$ ) of the photoaligned films of **1** as a function of temperature, perpendicular ( $\sigma_1$ ) and parallel ( $\sigma_2$ ) to the molecular axis of **1** (Figure 3b). In the SmA phase,  $\sigma_1$  is higher than  $\sigma_2$ . For example, the  $\sigma_1$  at 116 °C is  $3.1 \times 10^{-6}$  S cm<sup>-1</sup>, while the  $\sigma_2$  at 115 °C is  $3.9 \times 10^{-7}$  S cm<sup>-1</sup>. These results show that photoaligned thin films of **1** exhibit anisotropic ion conduction in the SmA phase.

Interestingly, anisotropic ion conduction is also observed in the photoaligned thin films of **1** in the N phase (Figure 3). The conductivities parallel to the molecular axis of **1** ( $\sigma_2$ ) significantly increase from  $5 \times 10^{-7}$  to  $1 \times 10^{-5}$  S cm<sup>-1</sup> during the SmA-N phase transition, while conductivities perpendicular to the molecular axis of **1** ( $\sigma_1$ ) drop to around  $10^{-6}$  S cm<sup>-1</sup>. These trends suggest that the 2D ionic pathways have been disrupted because of the phase transition to the N phase, but remarkably the molecules maintain their orientation, but not their position (Figure 3b). In the N phase, the ion transportation along the parallel direction of the molecular axis of **1** is higher than that perpendicular to the molecules axis (Figure 3). It is noteworthy that the anisotropy in the ion conduction changes during the SmA-N phase transition. The

ionic conductivities perpendicular to the molecular axis of **1** ( $\sigma_1$ ) are higher than those that are parallel ( $\sigma_2$ ), in the SmA phase. But, after heating to the N phase the conductivities parallel to the molecular axis of **1** ( $\sigma_2$ ) are higher than those perpendicular to the axis ( $\sigma_1$ ) (Figure 3). To the best of our knowledge, this behavior has not yet been reported.

In summary we have succeeded in applying efficient methodology for the homogeneous uniplanar alignment of ion conductive pathways for nanostructured materials. The new molecular design of **1** incorporating Azo groups allows the alignment of the LC domains via the photoinduced reorientation of the photochromic moiety. It is noteworthy that LC **1** exhibits anisotropic ion conduction in SmA and N phases. Thus, this new methodology for the alignment of layered ionic liquid crystals is promising because it allows the orientation of 2D ionic pathways perpendicular to the surface of the substrate, which is the most efficient organization for a practical application of electrolyte materials. Moreover, this concept has potential to be used in memory devices and to fabricate rewritable ionic circuits.

## ■ ASSOCIATED CONTENT

### 📄 Supporting Information

Detailed experimental procedures and results of characterization. This materials is available free of charge via the Internet at <http://pubs.acs.org>.

## ■ AUTHOR INFORMATION

### Corresponding Author

kato@chiral.t.u-tokyo.ac.jp

### Author Contributions

‡These authors contributed equally.

### Notes

The authors declare no competing financial interest.

## ■ ACKNOWLEDGMENTS

This study was partially supported by the Funding Program for World-Leading Innovative R&D on Science and Technology (FIRST) from the Cabinet Office, Government of Japan. This work was also partially supported by a Grant-in-Aid for Scientific Research (No. 22107003) in the Innovative Area of “Fusion Materials” (Area No. 2206) and Grant-in-Aid for The Global COE Program “Chemistry Innovation through Cooperation of Science and Engineering” from The Ministry of Education, Culture, Sports, Science and Technology (MEXT). E.U. is grateful for financial support from the Japan Society for the Promotion of Science (JSPS) Research Fellowship for Young Scientists.

## ■ REFERENCES

- (1) (a) Goodby, J. W.; Collings, P. J.; Kato, T.; Tschierske, C.; Gleeson, H.; Raynes, P. *Handbook of Liquid Crystals*, 2nd ed.; Wiley-VCH: Weinheim, 2014. (b) Kato, T. *Science* **2002**, *295*, 2414–2418. (c) Kerr, R. L.; Miller, S. A.; Shoemaker, R. K.; Elliott, B. J.; Gin, D. L. *J. Am. Chem. Soc.* **2009**, *131*, 15972–15973. (d) Chen, S.; Eichhorn, S. H. *Isr. J. Chem.* **2012**, *52*, 830–843. (e) Kato, T.; Mizoshita, N.; Kishimoto, K. *Angew. Chem., Int. Ed.* **2006**, *45*, 38–68. (f) Binnemans, K. *Chem. Rev.* **2005**, *105*, 4148–4204. (g) Rosen, B. M.; Wilson, C. J.; Wilson, D. A.; Peterca, M.; Imam, M. R.; Percec, V. *Chem. Rev.* **2009**, *109*, 6275–6540. (h) Wiggins, K. M.; Kerr, R. L.; Chen, Z.; Bielawski, C. W. *J. Mater. Chem.* **2010**, *20*, 5709–5714. (i) Noble, R. D.; Zhou, M. J.; Kidd, T. J.; Gin, D. L. *Adv. Mater.* **2005**, *17*, 1850–1853.

- (2) (a) Cho, B.-K.; Jain, A.; Gruner, S. M.; Wiesner, U. *Science* **2004**, *305*, 1598–1601. (b) Faul, C. F. J.; Antonietti, M. *Adv. Mater.* **2003**, *15*, 673–683. (c) Ikkala, O.; ten Brinke, G. *Science* **2002**, *295*, 2407–2409. (d) Houbenov, N.; Haataja, J. S.; Iatrou, H.; Hadjichristidis, N.; Ruokolainen, J.; Faul, C. F. J.; Ikkala, O. *Angew. Chem., Int. Ed.* **2011**, *50*, 2516–2520. (e) Cho, B.-K. *Polym. J.* **2012**, *44*, 475–489. (f) Zakrevskyy, Y.; Stumpe, J.; Faul, C. F. J. *Adv. Mater.* **2006**, *18*, 2133–2136. (g) Kumar, U.; Fréchet, J. M. J. *Adv. Mater.* **1992**, *4*, 665–667. (h) Thünnemann, A. F.; Kubowicz, S.; Burger, C.; Watson, M. D.; Tchebotareva, N.; Müllen, K. J. *Am. Chem. Soc.* **2003**, *125*, 352–356. (i) Ujiie, S.; Iimura, K. *Macromolecules* **1992**, *25*, 3174–3178. (j) Bazuin, C. G.; Guillon, D.; Skoulios, A.; Nicoud, J. F. *Liq. Cryst.* **1986**, *1*, 181–188.
- (3) (a) Yoshio, M.; Mukai, T.; Ohno, H.; Kato, T. *J. Am. Chem. Soc.* **2004**, *126*, 994–995. (b) Yoshio, M.; Kagata, T.; Hoshino, K.; Mukai, T.; Ohno, H.; Kato, T. *J. Am. Chem. Soc.* **2006**, *128*, 5570–5577. (c) Yoshio, M.; Ichikawa, T.; Shimura, H.; Kagata, T.; Hamasaki, A.; Mukai, T.; Ohno, H.; Kato, T. *Bull. Chem. Soc. Jpn.* **2007**, *80*, 1836–1841.
- (4) (a) Yoshio, M.; Mukai, T.; Kanie, K.; Yoshizawa, M.; Ohno, H.; Kato, T. *Adv. Mater.* **2002**, *14*, 351–354. (b) Hoshino, K.; Yoshio, M.; Mukai, T.; Kishimoto, K.; Ohno, H.; Kato, T. *J. Polym. Sci., Polym. Chem.* **2003**, *41*, 3486–3492.
- (5) (a) Ichikawa, T.; Yoshio, M.; Hamasaki, A.; Mukai, T.; Ohno, H.; Kato, T. *J. Am. Chem. Soc.* **2007**, *129*, 10662–10663. (b) Ichikawa, T.; Yoshio, M.; Hamasaki, A.; Taguchi, S.; Liu, F.; Zeng, X. B.; Ungar, G.; Ohno, H.; Kato, T. *J. Am. Chem. Soc.* **2012**, *134*, 2634–2643. (c) Hatakeyama, E. S.; Wiesenauer, B. R.; Gabriel, C. J.; Noble, R. D.; Gin, D. L. *Chem. Mater.* **2010**, *22*, 4525–4527. (d) Kutsumizu, S. *Isr. J. Chem.* **2012**, *52*, 844–853.
- (6) Kanazawa, A.; Ikeda, T.; Abe, J. *J. Am. Chem. Soc.* **2001**, *123*, 1748–1754.
- (7) Shimura, H.; Yoshio, M.; Hamasaki, A.; Mukai, T.; Ohno, H.; Kato, T. *Adv. Mater.* **2009**, *21*, 1591–1592.
- (8) Iinuma, Y.; Kishimoto, K.; Sagara, Y.; Yoshio, M.; Mukai, T.; Kobayashi, I.; Ohno, H.; Kato, T. *Macromolecules* **2007**, *40*, 4874–4878.
- (9) (a) Kato, T. *Angew. Chem., Int. Ed.* **2010**, *49*, 7847–7848. (b) Soberats, B.; Yoshio, M.; Ichikawa, T.; Taguchi, S.; Ohno, H.; Kato, T. *J. Am. Chem. Soc.* **2013**, *135*, 15286–15289. (c) Kimura, K.; Suzuki, T.; Yokoyama, M. *J. Phys. Chem.* **1990**, *94*, 6090–6093. (d) Keplinger, C.; Sun, J. Y.; Foo, C. C.; Rothmund, P.; Whitesides, G. M.; Suo, Z. G. *Science* **2013**, *341*, 984–987. (e) Lowe, A. M.; Abbott, N. L. *Chem. Mater.* **2011**, *24*, 746–759. (f) Wiesenauer, B. R.; Gin, D. L. *Polym. J.* **2012**, *44*, 461–468.
- (10) (a) Kaneshige, M.; Tokuhisa, H.; Yokoyama, M.; Kimura, K. *J. Polym. Sci., Polym. Chem.* **1993**, *31*, 2809–2813. (b) Morooka, H.; Yokoyama, M.; Kimura, K. *J. Appl. Polym. Sci.* **1991**, *43*, 1233–1239. (c) Tan, B. H.; Yoshio, M.; Ichikawa, T.; Mukai, T.; Ohno, H.; Kato, T. *Chem. Commun.* **2006**, 4703–4705.
- (11) (a) Aprahamian, I.; Yasuda, T.; Ikeda, T.; Saha, S.; Dichtel, W. R.; Isoda, K.; Kato, T.; Stoddart, J. F. *Angew. Chem., Int. Ed.* **2007**, *46*, 4675–4679. (b) Baranoff, E. D.; Voignier, J.; Yasuda, T.; Heitz, V.; Sauvage, J. P.; Kato, T. *Angew. Chem., Int. Ed.* **2007**, *46*, 4680–4683. (c) Baranoff, E. D.; Voignier, J.; Yasuda, T.; Heitz, V.; Sauvage, J. P.; Kato, T. *Mol. Cryst. Liq. Cryst.* **2009**, *509*, 907–914. (d) Saez, I. M.; Goodby, J. W. *Struct. Bonding (Berlin)* **2008**, *128*, 1–62.
- (12) (a) Ichimura, K.; Suzuki, Y.; Seki, T.; Hosoki, A.; Aoki, K. *Langmuir* **1988**, *4*, 1214–1216. (b) Ikeda, T. *J. Mater. Chem.* **2003**, *13*, 2037–2057. (c) Kawatsuki, N. *Chem. Lett.* **2011**, *40*, 548–554. (d) Ichimura, K. *Chem. Rev.* **2000**, *100*, 1847–1874. (e) Seki, T.; Morikawa, Y.; Uekusa, T.; Nagano, S. *Mol. Cryst. Liq. Cryst.* **2009**, *510*, 21–33. (f) Yu, H. F.; Ikeda, T. *Adv. Mater.* **2011**, *23*, 2149–2180. (g) Natansohn, A.; Rochon, P. *Chem. Rev.* **2002**, *102*, 4139–4176.
- (13) (a) Zakrevskyy, Y.; Stumpe, J.; Smarsly, B.; Faul, C. F. J. *Phys. Rev. E* **2007**, *75*, 031703. (b) Xiao, S.; Lu, X.; Lu, Q.; Su, B. *Macromolecules* **2008**, *41*, 3884–3892. (c) Xiao, S.; Lu, X.; Lu, Q. *Macromolecules* **2007**, *40*, 7944–7950.
- (14) (a) Kempe, C.; Rutloh, M.; Stumpe, J. *J. Phys.: Condens. Matter.* **2003**, *15*, S813–S823. (b) Uchida, E.; Shiraku, T.; Ono, H.; Kawatsuki, N. *Macromolecules* **2004**, *37*, 5282–5291. (c) Kawatsuki, N.; Shiraku, T.; Uchida, E. *Mol. Cryst. Liq. Cryst.* **2005**, *441*, 163–171.
- (15) Thin film of **1** was exposed to nonpolarized 365 nm UV light irradiation (250 mW/cm<sup>2</sup>) for 10–20 min and linearly polarized (LP) 540 nm light (80 mW/cm<sup>2</sup>) irradiation for 10 min. The direction of the polarizer determined the orientation of Azo groups. All the processes were conducted at rt, and then the film was annealed for 10 min at 100 °C before the measurements.
- (16) Ionic conductivities were measured by using the alternating current impedance method.